Biochimie 144 (2018) 74–84

Contents lists available at ScienceDirect

Biochimie

journal homepage: www.elsevier.com/locate/biochi

Research paper

Why do antifreeze proteins require a solenoid?

M. Banach [a], L. Konieczny [b], I. Roterman [a, *]

[a] Department of Bioinformatics and Telemedicine, Jagiellonian University, Medical College, Lazarza 16, 31-530, Krakow, Poland
[b] Chair of Medical Biochemistry, Jagiellonian University, Medical College, Kopernika 7, 31-034, Krakow, Poland

ARTICLE INFO

Article history:
Received 18 August 2017
Accepted 12 October 2017
Available online 17 October 2017

Keywords:
Hydrophobicity
Antifreeze proteins
Solenoid
Amyloid

ABSTRACT

Proteins whose presence prevents water from freezing in living organisms at temperatures below 0 °C are referred to as antifreeze proteins. This group includes molecules of varying size (from 30 to over 300 aa) and variable secondary/supersecondary conformation. Some of these proteins also contain peculiar structural motifs called solenoids. We have applied the fuzzy oil drop model in the analysis of four categories of antifreeze proteins: 1 – very small proteins, i.e. helical peptides (below 40 aa); 2 – small globular proteins (40–100 aa); 3 – large globular proteins (>100 aa) and 4 – proteins containing solenoids. The FOD model suggests a mechanism by which antifreeze proteins prevent freezing. In accordance with this theory, the presence of the protein itself produces an ordering of water molecules which counteracts the formation of ice crystals. This conclusion is supported by analysis of the ordering of hydrophobic and hydrophilic residues in antifreeze proteins, revealing significant variability – from perfect adherence to the fuzzy oil drop model through structures which lack a clearly defined hydrophobic core, all the way to linear arrangement of alternating local minima and maxima propagating along the principal axis of the solenoid (much like in amyloids). The presented model – alternative with respect to the ice docking model – explains the antifreeze properties of compounds such as saccharides and fatty acids. The fuzzy oil drop model also enables differentiation between amyloids and antifreeze proteins.

1. Introduction

The role of antifreeze proteins cannot be properly analyzed without a discussion of the structuralization of water itself. Numerous publications exist where the structure of ice is discussed, starting with Bernal-Fowler rules [1–9]. In fact, structuralization of ice is a far more popular study subject than that of liquid water in the presence of dissolved compounds [10–17]. Ben Naim in Ref. [18] proposes an iceberg model to explain the ordering of water molecules. Our work approaches structuralization of water from the perspective of its effects on other molecules. In particular, surfactant micelles where hydrophobicity is concentrated in the central portion of the micelle while polar structures remain exposed, can only emerge in the presence of water [19]. Polypeptide chain folding appears to result from a similar active influence of the water environment. Altering the properties of this environment triggers structural changes, affecting the ultimate conformation of the protein – for example, in the case of elastin [20]. In contrast to individual surfactant molecules, the polypeptide chain exhibits variable hydrophobicity. The oil drop model [21] predicts concentration of hydrophobic residues at the core of the protein, along with exposure of hydrophilic residues on the surface (where they remain in contact with water). This is regarded as a consequence of water acting on individual fragments of the target chain. This simplistic model has since been extended, resulting in the so-called fuzzy oil drop model, where the distribution of hydrophobicity in a protein is modeled by a 3D Gaussian. A detailed description of the fuzzy oil drop model can be found in Ref. [22], where the authors show consistent results regardless of the applied intrinsic hydrophobicity scale. The β-strand has long been known for its association with amyloid-like and amyloid forms, including solenoids [23–25]. Solenoids themselves are categorized on the basis of such parameters as handedness, twist angle, oligomerization state and coil shape [26]. Proteins which contain repeated sequences are strongly predisposed towards generation of solenoid (or solenoid-like) conformations. This fact has led researchers to assemble a database of tandem repeated structure proteins [27,28]. Factors which determine linear deformations in solenoids compared to the so-called horseshoe structure are discussed in Ref. [29]. Antifreeze

* Corresponding author.
E-mail address: myroterm@cyf-kr.edu.pl (I. Roterman).

https://doi.org/10.1016/j.biochi.2017.10.011

proteins are described in numerous publications, some of which suggest that their mechanism of action is based on docking of ice crystals [30–32].

2. Materials and methods

2.1. Data

Table 1 lists proteins which have been subjected to analysis. This set was obtained by scanning the PDB database using the "antifreeze" keyword. Proteins were divided into groups depending on their size. Particular attention was devoted to solenoid structures which are present in some of the analyzed proteins.

Since all proteins selected for analysis are the antifreeze proteins, it is difficult to distinguish each of them. This is why the PDB IDs are treated as "names" of proteins.

2.2. Programs

All parameters were calculated using custom software. Identification of domains and secondary folds follows the PDBSum classification [60].

2.3. Fuzzy oil drop model

A detailed introduction to the fuzzy oil drop model can be found in Ref. [22] Below we provide a brief recapitulation of the model's basic concepts insofar as they relate to the presented work. The general principle is that the observed hydrophobicity distribution in the target molecule (denoted O), which results from inter-residue interactions [61], is compared to the so-called idealized (or theoretical) distribution (denoted T), mathematically expressed by a 3D Gaussian. Quantitative comparison of both distributions is based on the concept of divergence entropy [62]. The resulting similarity measure depends on the length of the input chain. Additionally, since the obtained value represents entropy, it may not be interpreted on its own, but must instead be compared to another boundary distribution, which we refer to as unified (R). In this distribution, each residue is ascribed the same hydrophobicity value of 1/N, where N is the number of residues in the input chain. To avoid having to work with two distinct parameters, i.e. observed-vs.-theoretical and observed-vs.-unified entropy (O|T and O|R respectively), we derive an additional coefficient referred to as Relative Distance (RD):

$$RD = \frac{O|T}{O|T + O|R}$$

$O|T$, $O|R$ and RD may be computed for any arbitrarily selected structural unit: protein complexes, individual proteins and specific domains. In each case, a different encapsulating ellipsoid, custom-tailored for the target unit, must be prepared. Additionally, when considering specific parts of the protein chain, O_i, T_i and R_i values must be renormalized so that their sum is always equal to 1. This process enables us to identify regions which exhibit good accordance with the model and therefore contribute to tertiary structural stabilization.

Fig. 1 provides a visual description of a representative case.

RD tells us whether the molecule contains a well-ordered hydrophobic core (RD < 0.5) or lacks such a core (RD > 0.5). The threshold value of 0.5 was selected since the distance comparison is relative in scope. Simply speaking, RD < 0.5 means that the molecule more closely resembles the idealized Gaussian distribution than the unified distribution, while the opposite is true when RD > 0.5.

It should be noted that similar analysis can be performed for selected fragments of the protein. In such cases, the 3D Gaussian is plotted for the specific unit (domain, chain, complex) and a new value of RD is calculated following prior normalization of O_i, T_i and R_i. This value expresses the status of the given unit within the framework of the larger structure to which it belongs. For example, in this work we compute RD coefficients for solenoid fragments and for selected secondary folds.

3. Results

The results of our analysis are summarized by a set of RD values calculated for complexes, individual proteins and selected domains (where applicable). Since antifreeze proteins vary in length, we further subdivided this class into groups, as shown in Table 2. For each group, several representative cases were singled out for detailed analysis, which involved computing RD values for individual secondary folds, plotting T and O distributions in a manner which enables visual comparison, and presenting 3D images of each target protein.

The presented proteins exhibit significant conformational variability – this is reflected by variable presentation of results, depending on the complexity of the given structure.

3.1. Peptides – length below 40 aa

This set of proteins represents structural forms which are essentially helical. The chain length is too short to enable generation of tertiary structures. Applying the hydrophobic core drop model to individual helices is questionable on theoretical grounds; however, mindful of the aim of presenting a holistic description of all types of antifreeze proteins, we have calculated FOD parameters for these proteins as well. Table 2 lists the corresponding RD values. Only 2LQ0, a *de novo* protein, remains accordant with the theoretical distribution – however, it should be noted that this protein was synthesized with the specific goal of retaining a centralized hydrophobicity peak. No naturally occurring category I antifreeze proteins exhibit similar properties. Fig. 2 highlights the differences between T and O for two representative polypeptides.

The *de novo* protein (2LQ0) contains hydrophilic residues in its

Table 1
Set of proteins subjected to analysis, assigned to distinct groups depending on their size. Brief structural characteristics are also listed for each group. Underlined identifiers correspond to proteins which have been selected for detailed presentation.

Length	Structure	PDB ID and references
<40 aa	Loose helices	1J5B [33], 1Y03 [34], 2LQ0 [35]
40 aa< <100 aa	Globular	1B7I [36], 3NLA [37], 1KDE [38], 2LX2 [39]
100 aa <	Globular, complexes	2PY2 [40], 1C3Y [41], 4KDV [42], 1C89 [43], 2ZIB [44]
100 aa <	Solenoid complexes	1EWW [45],1L0S [46],1L1I [47],1M8N [48], 1N4I [49], 1Z2F [50],2PNE [51], 3BOG [51], 3P4G [52], 3ULT [53]
100 aa <	Solenoid with helix complexes	3UYU [54],3VN3 [55],3WP9 [56],4NU2 [57],4NUH [57],5B5H [58]
100 aa <	Amyloid-like	4DT5 [59]

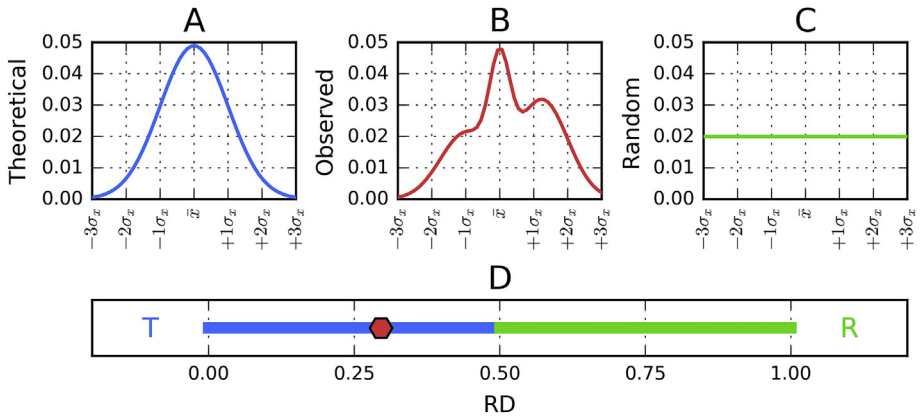

Fig. 1. Relation between the observed (B) and reference (A; C) distributions of hydrophobicity, along with the corresponding value of RD (0.296), plotted on a horizontal axis (D). The red mark represents the status of the hypothetical protein undergoing analysis. In this case, the observed distribution of hydrophobicity is consistent with the theoretical model, i.e. a monocentric hydrophobic core is present in the protein. The presentation has been reduced to a single dimension for the sake of clarity.

Table 2
RD values for proteins with chain length below 40 aa (purely helical forms). Underlined identifiers correspond to proteins which are described in more detail.

PDB ID	RD	Length	Source organism
1J5B	0.767	38 aa	Synthetic polypeptide – sequence taken from *Pseudopleuronectes americanus*
1Y03	0.777	35 aa	*Myoxocephalus scorpius*
2LQ0	0.191	25 aa	*De novo* design

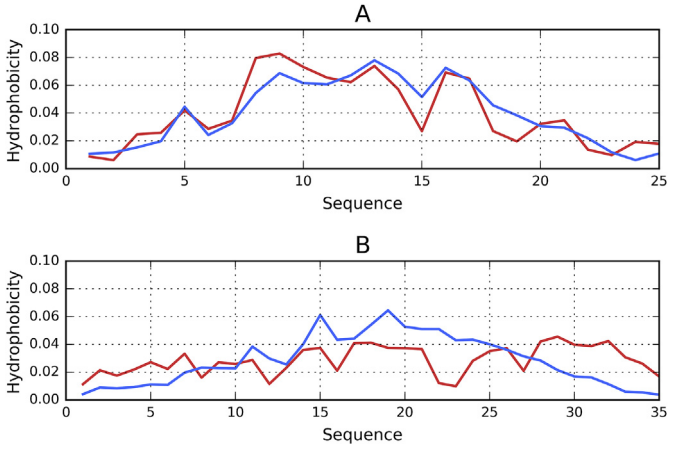

Fig. 2. Comparison of theoretical (T - blue) and observed (O - red) hydrophobicity profiles in 2LQ0 (accordant protein; A) and 1Y03 (discordant protein; B). Quantitative analysis of the differences between individual profiles is provided in Table 2.

terminal sections and hydrophobic residues in the central section. This results in good accordance with the theoretical model, even though no actual hydrophobic "core" is present.

The relation between the FOD status of each protein and its influence on the water environment will be discussed jointly in further sections.

The presented proteins differ with regard to their adherence to the fuzzy oil drop model. Comparing T and O distributions for 2LQ0 (Fig. 2A) reveals good accordance, since hydrophobicity is high in the central section of the chain and low in the terminal sections. This indicates that a central hydrophobic core is present – as indeed predicted by the fuzzy oil drop model. Close correspondence between T and O can be seen, with only limited differences for certain individual residues.

In contrast, the observed hydrophobicity in 1Y03 (Fig. 2B) is greater than expected in the terminal sections and lower in the central section, indicating that the protein as a whole diverges from the model and does not contain a monocentric hydrophobic core.

It should be noted that referring to a "hydrophobic core" in a very short protein which consists entirely of an elongated helix is questionable on theoretical grounds, since such proteins lack a tertiary conformation. Nevertheless, the fuzzy oil drop model may be applied to such cases for comparative purposes.

3.2. Small proteins – polypeptide chain length 60–80 aa

This group comprises globular antifreeze proteins with chain length between 60 and 100 aa, as listed in Table 3.

Representative theoretical and observed distributions for two selected proteins – 1B7I and 3NLA – reveal good accordance between both profiles (Fig. 3). This means that hydrophilic residues are exposed on the surface while hydrophobic residues are concealed inside, shielded from the environment. Consequently, both proteins are highly soluble and do not easily interact with other molecules. The ability to bind ligands would require a suitable cavity (characterized by lower-than-expected hydrophobicity), while complexation capabilities would call for excess hydrophobicity on the surface. No such properties are observed in either 1B7I or 3NLA. In the latter case, from among 40 models listed in PDB,

Table 3
RD parameters for antifreeze proteins with chain length between 50 and 80 aa. Pairs of values reflect the status of PDB models for which RD attains the lowest and greatest value respectively. Minimum and maximum values are listed for structures deposited in PDB in the form of sets (NMR technique applied). Underlined identifiers correspond to proteins which are described in more detail.

PDB ID	RD	Length	Source organism
1B7I	0.289	66 aa	*Macrozoarces americanus*
3NLA	0.502–0.371	73 aa	*Lycodichthys dearborni*
1KDE	0.296–0.331	65 aa	*Macrozoarces americanus*
2LX2	0.303–0.321	67 aa	*Zoarces elongatus*

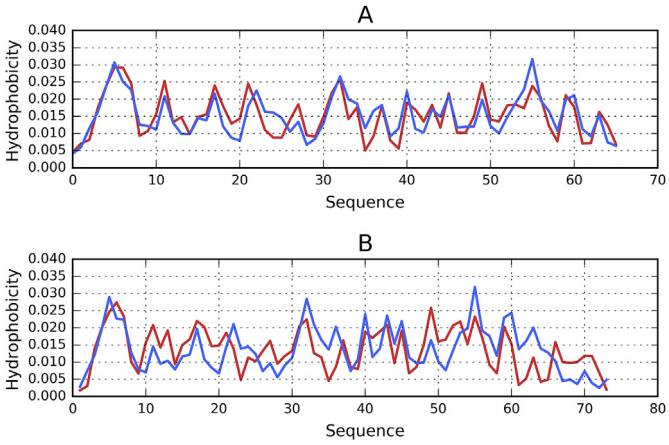

Fig. 3. Theoretical (T - blue) and observed (O - red) hydrophobicity for two proteins: A – 1B7I, B – 3NLA. Good accordance between T and O is observed in both cases (local discrepancies in the C-terminal fragment of 3NLA notwithstanding).

only two exhibit RD greater than 0.5 – we thus believe that this marginal violation of the limit may be overlooked.

Exposure of polar residues (carrying charge) doubtlessly exerts an influence on the structuralization of water in direct proximity of the protein. The polar surface represents a *quasi* matrix for the surrounding aqueous environment. The resulting structural effects likely propagate beyond the layer directly adjacent to the molecular surface, counteracting formation of ice crystals in a certain radius around the protein.

Much like in Fig. 2A, the red and blue lines are closely aligned, with only marginal differences between both distributions (O and T).

3.3. Proteins with chain length above 100 aa

Table 4 lists RD values for proteins where the chain length is greater than 100 aa.

Proteins with chains longer than 100 aa (but not longer than 150 aa) tend to adopt globular conformations, with a clearly defined hydrophobic core. This ordering is also evident in individual domains (see 1C89).

Fig. 4 presents two sample proteins: 1C3Y (A – conformant) and 1C89 (B – discordant). While 1C3Y contains a monocentric hydrophobic core, in 1C89 no concentration of hydrophobicity at the geometric center is observed since the protein consists of two loosely linked domains. The flexible nature of the linker results in good mobility of both domains with respect to each other. This is consistent with the observation that increased flexibility decreases antifreeze activity (understood as the ability to bind ice) [63].

The structure of 2ZIB diverges from fuzzy oil drop model predictions. Notably, this relatively small protein (130 aa) contains five disulfide bonds. From the perspective of the FOD model, such bonds may either "cooperate" with hydrophobic forces by reinforcing a monocentric hydrophobic core, or stabilize the protein in a discordant state, where no monocentric core is present [64]. 2ZIB appears to represent the latter category.

The presence of so many SS bonds which disrupt the natural core structure means that the positions of individual residues do not reflect the hydrophobicity they carry. As a result, exposure of hydrophobic residues on the protein surface may alter the ordering of water molecules in their proximity.

The distributions plotted in Fig. 4A may be interpreted as follows: in the theoretical distribution local maxima indicate residues which comprise the hydrophobic core, while local minima correspond to residues found on the protein surface. The red line (observed distribution) is generally consistent with this model, with some marginal discrepancies (e.g. in the 50–60 range). Unlike 1C3Y, in 1C89 there are significant deviations in areas where high hydrophobicity is expected, indicating that this protein does not contain a central hydrophobic core. Visual inspection appears to suggest that 1C3Y conforms to the model while 1C89 diverges from it. This observation is confirmed by objective analysis of RD coefficients (Table 4).

3.4. Solenoids

Arguably the most interesting group of antifreeze proteins consists of structures which contain solenoid folds (Table 5). These proteins vary in size (between 100 and 300 aa) and include multi-domain and multi-chain complexes. Note that solenoids are not specific to antifreeze proteins – they are present in numerous other proteins with varying biological characteristics.

Table 5 lists RD values for antifreeze proteins which contain solenoid folds.

Table 5 lists RD values for entire molecules, for individual solenoid fragments and for their terminal sections. In some cases the solenoid terminates without a bounding "cap".

Table 4
RD values for proteins with chain length beyond 100 aa. Underlined identifiers correspond to proteins which are described in more detail.

PROTEIN PDB ID Chains Domains	RD	Length	Source organism
2PY2 – complex	**0.792**	6 × 127	*Clupea harengus*
Chain A	0.479	127	
Chain B	0.481	127	
Chain C	0.484	127	
Chain D	0.472	127	
Chain E	0.479	127	
Chain F	0.427	127	
Domain	0.425–0.435	106	
1C3Y	0.381	108	*Tenebrio molitor*
4KDV	**0.659**	102	*Marinomonas primoryensis*
1C89	**0.636–0.708**	134	*Pachycara brachycephalum*
Domain 1-66	0.290–0.355	66	
Domain 71-134	0.327–0.380	64	
2ZIB II	**0.536**	130	*Brachyopsis rostratus* 5SS

Values given in bold distinguish the status of hydrophobic core recognised as disordered (not accordant with the idealised distribution).

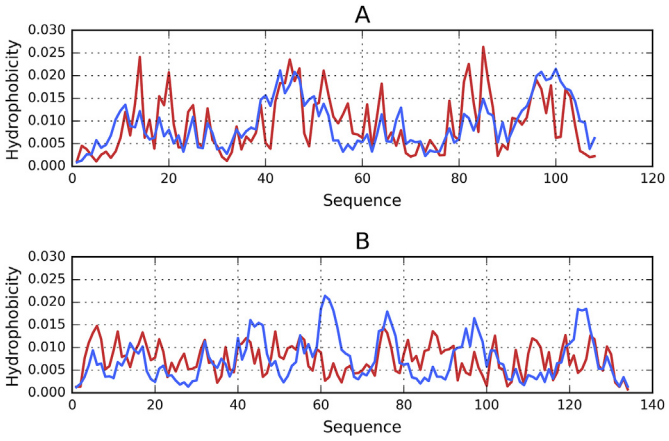

Fig. 4. Relation between the theoretical (blue) and observed (red) hydrophobicity profiles in 1C3Y (A – accordant) and 1C89 (B – discordant).

Table 5
RD values for proteins which contain solenoid folds. Values are listed separately for protein complexes, individual chains and domains (where applicable), for solenoid fragments and for their N- and C- terminal fragments which act as "stop" signals, preventing unchecked propagation.*** – amyloid-like protein. Underlined identifiers correspond to proteins which are described in more detail.

PROTEIN PDB ID and source organism	RD	SOLENOID	N-terminal	C-terminal
1EWW	0.438–**0.538**-	0.488	0.297	0.451
Choristoneura fumiferan				
1L0S – complex	**0.800**			
Choristoneura fumiferana				
Chain A	**0.526**	**0.502**	0.479	0.499
Chain B	**0.521**	0.459	0.487	0.499
Chain C	**0.529**	0.482	0.464	0.492
Chain D	**0.525**	0.472	**0.508**	**0.510**
D1	0.277–0.330			
1L1I	**0.552**	0.481	0.346	0.211
Tenebrio molitor				
1M8N	**0.784**			
Choristoneura fumiferana				
Chain A	**0.656**	**0.594**	0.403	0.485
Chain B	**0.675**	**0.596**	**0.595**	0.481
Chain C	**0.675**	**0.594**	**0.589**	0.485
Chain D	**0.653**	**0.561**	0.372	0.467
1N4I	0.480–**0.520**	0.403	0.408	0.441
Choristoneura fumiferana				
1Z2F	**0.671**	**0.570**	0.473	**0.597**
Choristoneura fumiferana				
2PNE	**0.665**	**0.665**		
Hypogastrura harveyi				
3BOG	**0.693**	**0.693**		
Hypogastrura harveyi				
Chain A	**0.654**	**0.654**		
Chain B	**0.671**	**0.671**		
Chain C	0.327	0.327		
Chain D	0.305	0.305		
3P4G – complex	**0.820**			
Marinomonas primoryensis				
Chain A	**0.753**	**0.745**	0.393	0.374
Chain B	**0.745**	**0.732**	0.091	0.466
Chain C	**0.749**	**0.737**	0.230	0.358
Chain D	**0.762**	**0.750**	0.367	0.423
3ULT***	**0.729**			
Lolium perenne				
Chain A	**0.674**	0.432	**0.640**	0.401
Chain B	**0.700**	0.496	**0.692**	0.375

Values given in bold distinguish the status of hydrophobic core recognised as disordered (not accordant with the idealised distribution).

The vast majority of solenoid-containing proteins (in fact, nearly all of them) exhibit RD much greater than 0.5. This means that such proteins do not contain monocentric hydrophobic cores encapsulated by hydrophilic shells (Fig. 5). This divergence can be attributed to alternative distributions of hydrophobicity throughout the protein body. In solenoid fragments, local hydrophobicity minima and maxima ted to propagate linearly along the principal axis of the solenoid.

This observation is supported by comparison of theoretical and observed hydrophobicity distribution profiles (see Fig. 5), which reveal large discordances. Where solenoids are present, no significant concentration of hydrophobicity can be observed in the central part of the protein. Instead, the structure is dominated by local effects, and specifically by the intrinsic hydrophobicity of each participating residue. Such local distribution of hydrophobicity repeats itself in each β-strand belonging to the solenoid, resulting in linear propagation of alternating peaks (maxima) and troughs (minima). This phenomenon effectively prevents formation of a monocentric hydrophobic core. Correlation coefficients calculated for the solenoid section in 1M8N-B are as follows: O/H (observed vs. intrinsic hydrophobicity, using the scale proposed in Ref. [22]): 0.822; O/T (observed vs. theoretical hydrophobicity): 0.270; H/T (intrinsic vs. theoretical hydrophobicity): 0.328 (see Fig. 6). This means that the folding process is driven by individual properties of each amino acid (high O/H coefficient) rather than by the molecule-wide tendency to produce a common hydrophobic core (low O/T coefficient).

Since linear propagation is – in principle – unbounded, evolution has equipped solenoids with special "stoppers" on either end. These terminal fragments prevent excessive growth of the solenoid by introducing a local distribution of hydrophobicity which is consistent with the fuzzy oil drop model. One side of each cap faces the water environment, exposing polar residues, while the opposite side remains compatible with the solenoid. In some cases a single cap is sufficient: complexation of such solenoids produces a dimer which is capped on both ends, mitigating the danger of unchecked propagation (such as in amyloids).

It further appears that, by exposing a large surface area dominated by alternating bands of hydrophobicity and hydrophilicity the solenoid affects the water environment, forcing the surrounding water molecules to also arrange themselves into matching "bands". This would disrupt the natural ordering required for an ice crystal to emerge.

The β-roll fold structure of 3ULT deserves particular attention. This type of conformation closely resembles an amyloid (assuming that amyloids are characterized by linear propagation of local hydrophobicity minima and maxima – as discussed in Refs. [30,31]). 3ULT is not, however, an amyloid. The presence of a centralized

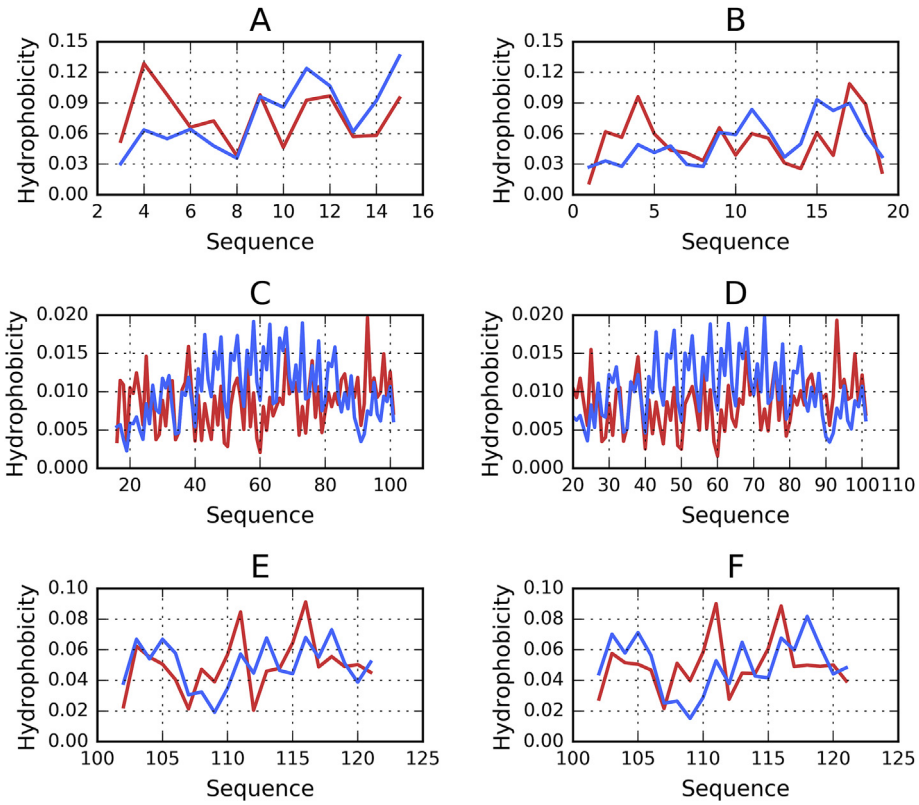

Fig. 5. Sample T (blue) and O (red) profiles for proteins which contain solenoid fragments. 1M8N-B A – N-terminal fragment 3-15, C – solenoid 16-101, D – C-terminal fragment 102-121 1Z2F – B – N-terminal fragment 1-19, D – solenoid 20-101, E – C-terminal fragment 102-121.

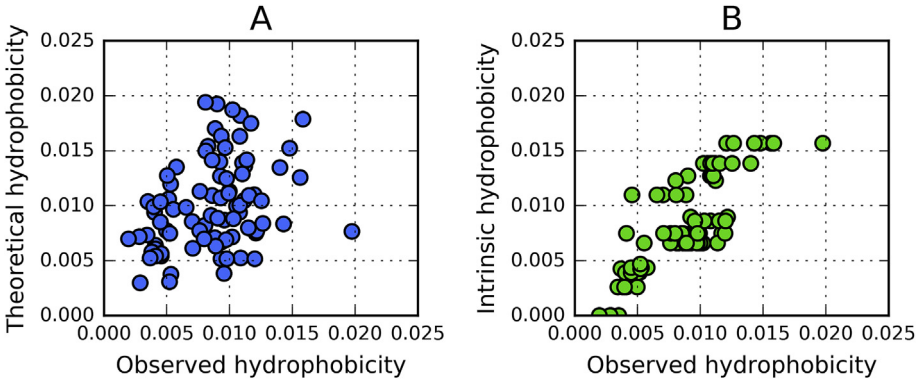

Fig. 6. Left-hand diagram: relation between observed (horizontal axis) and theoretical (vertical axis) hydrophobicity; right-hand diagram: relation between observed (horizontal axis) and intrinsic (vertical axis) hydrophobicity as it appears in 1M8N-B. Intrinsic hydrophobicity has been calculated by applying the scale proposed in [22].

local hydrophobicity peak means that the solenoid section is locally consistent with the FOD model. Additionally, exposed loops are all composed of hydrophilic residues, which conforms to the 3D Gaussian distribution.

Fig. 7 illustrates the placement of the hydrophobic band in 3ULT. The central portion of the solenoid constitutes a “quasi” hydrophobic core, while the surrounding loops ensure entropically advantageous contact with water.

Linear propagation (consistent recurrence of strongly hydrophobic residues every 7–10 aa) facilitates elongation of the solenoid. Here, adherence to the fuzzy oil drop model is associated with centralized placement of hydrophobic residues (mostly Val).

This example clearly illustrates the differences between an amyloidogenic solenoid and a linear form which does not support

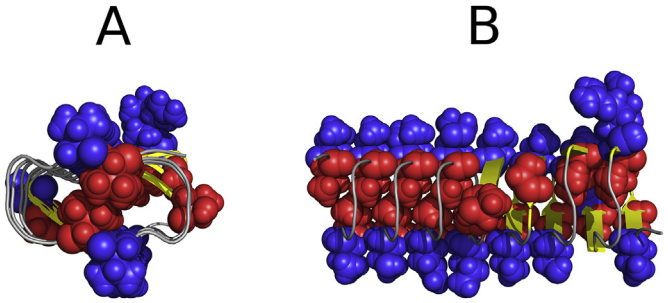

Fig. 7. Structure of the A chain of 3ULT in two planes (A and B). Red spheres correspond to hydrophobic residues while blue loops are comprised by hydrophilic residues.

formation of elongated fibrils. FOD analysis indicates that the C-terminal fragment remains consistent with the model, effectively capping the protein and preventing unchecked growth. Accordance of this fragment with FOD model reveals its role as stopper representing differentiated distribution in the C-terminal fragment. Its hydrophobicity distribution matches the distribution present in the solenoid, while – on the opposite side – the C-terminal fragment exposes low hydrophobicity, adequate for interaction with water. This is what prevents unlimited elongation of the solenoid.

The distribution illustrated in Fig. 7 also suggests what potential effect the protein may exert on the surrounding water. Recurring rounded loops comprised of hydrophilic residues attract water dipoles and introduce a structural model which disfavors formation of ice crystals.

Such arrangement does not preclude complexation of ice, as suggested in numerous publications [13,16,17,44,45]; however, based on the presented analysis we may conclude that 3ULT definitely affects the structuralization of water in its neighborhood. Similar linear propagation is observed in 3P4G, and particularly in its two β-sheets. Fig. 8 illustrates the distribution of hydrophobicity in this protein. Observed hydrophobicity adopts a sinusoidal pattern along the entire chain. RD values calculated separately for each of two β-sheets comprising the solenoid are 0.787 and 0.738 respectively. Clear deviations from the globular distribution can be observed (particularly in terminal sections, where low hydrophobicity is expected); additionally, no monocentric hydrophobic core is present. The similarity between the observed and intrinsic hydrophobicity distribution suggests that the conformation of the molecule is determined by local effects.

The theoretical distribution (blue – Fig. 8) exhibits a clearly defined hydrophobicity peak in the central part of the solenoid, along with low hydrophobicity in the terminal sections. Neither the observed (red) nor the intrinsic (green) distributions correspond to this model – instead, they resemble sinusoids, suggesting linear propagation of low and high hydrophobicity bands along the solenoid's axis.

Profiles shown in Fig. 8 are the perfect examples of fuzzy oil drop model application which are easy to interpret. The blue line represents the almost ideal, expected Gaussian distribution with high concentration of hydrophobicity in the central part of molecule – central part of solenoid. Red line shows the observed distribution which does not follow the idealized one. Neither central high concentration nor the near zero level on the N-and C-terminal fragments are observed. To search for the source of this disobedience (in respect to idealized model) the distribution of intrinsic hydrophobicity is shown (green line). The obvious high accordance between observed and intrinsic hydrophobicity reveals the later one as the main factor influencing the construction of the final hydrophobicity distribution. This example is in contrast to the profiles shown in Fig. 4A where the observed distribution almost follows the expected one. The status of hydrophobic distribution in 3P4G can be called as “selfish” one as not participating in the construction of the centric hydrophobic core common for entire molecule. The “selfish” distribution can be understood also as following the individual hydrophobic preferences.

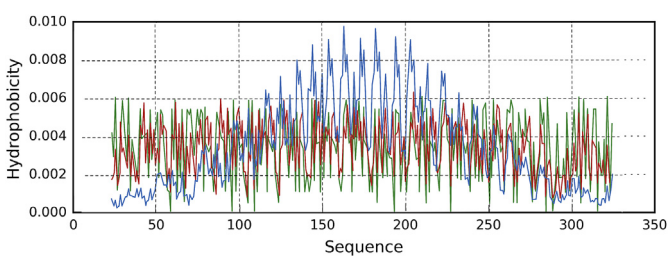

Fig. 8. Theoretical (blue), observed (red) and intrinsic (green) hydrophobicity distributions in 3P4G.

The repeatability of the sinusoid-like form of observed (and intrinsic) hydrophobicity distribution visualizes the structural repeatability as it occurs in solenoid.

3.5. Solenoid + helix

Some antifreeze proteins are characterized by the presence of a solenoid along with a parallel helix. In order to explain the role of this helix, we carried out FOD analyses of the relevant fragment. Results are summarized in Table 6.

This group of proteins is characterized by high RD values, suggesting that no monocentric core is present. All solenoid fragments also exhibit high RD – a consequence of linear propagation of hydrophobicity minima and maxima. All “stop” sections remain consistent with the model, which corresponds to their function (preventing unbounded propagation of the solenoid).

The accompanying helix remains highly consistent with the theoretical distribution and likely contributes to solubility of the analyzed proteins. One exception is 4NUH, where the helix diverges from FOD predictions, but a separate fragment – parallel to both the helix and the solenoid – remains accordant (value marked with an asterisk in Table 6) and may play a stabilizing role with regard to the surrounding water environment.

Another interesting study case is 4DT5 (Fig. 9). In the presented group, this protein most closely resembles an amyloid fibril, with consistent propagation of an identical geometric pattern and no loose loops between successive β-strands. Such linear propagation of local minima and maxima, devoid of any discernible hydrophobic core, becomes evident when comparing theoretical and observed hydrophobicity distribution profiles. The diagrams also highlight the status of terminal fragments, which remain locally consistent with the model and therefore “cap” the solenoid, preventing unbounded elongation.

Analysis of T and O distributions (Fig. 9 – note the yellow and orange bands bracketed by two black vertical bars) suggests that the observed distribution in β-structural fragments deviates from the theoretical model in favor of a sinusoid form. This is particularly evident in the 20–40 fragment where the observed distribution is almost a polar opposite of the theoretical distribution. This confirms linear propagation of a local conformational pattern.

4. Conclusions and discussion

The presented work suggests a mechanism of action for antifreeze proteins and highlights the differences between such proteins and amyloids. A protein which conforms to the 3D Gaussian distribution of hydrophobicity exposes its hydrophilic residues on the surface (where values of the Gaussian become close to 0). This means that the protein surface is strewn with charges – both positive and negative. Such exposure exerts an influence on water dipoles which align themselves perpendicularly to the surface. This phenomenon is not restricted to the layer immediately adjacent to the surface, but cascades onto further layers (although we do not currently know its range).

If the protein is disordered (e.g. short helices) and dominated by the intrinsic properties of individual residues then the neighboring water molecules will adapt to the chaotic distribution of surface charge. The resulting structure cannot be accurately determined, but likely differs from the one described above, where the entire surface is composed of polar residues.

Large proteins which diverge from the theoretical Gaussian

Table 6
RD status of proteins which contain a solenoid along with a parallel helix. "N-terminal STOP" and "C-terminal STOP" refer to N- and C-terminal fragments which bracket the solenoid section.* - additional fragment (2–14) parallel to both the solenoid and the helix.

PROTEIN	RD				
	Chain	N-terminal STOP	C-terminal STOP	Solenoid	Helix
3UYU-compl.	**0.781**				
Leucosporidium					
Chain A	**0.602**	0.297	0.367	**0.660**	0.477
Chain B	**0.597**	0.331	0.342	**0.656**	0.470
3VN3-compl.	**0.803**				
Typhula ishikariensis					
Chain A	**0.714**	**0.709**	0.288	**0.736**	0.469
Chain B	**0.700**	**0.679**	0.253	**0.720**	0.434
3WP9	**0.658**	0.168	0.430	**0.678**	0.487
Colwellia					
4NU2	**0.670**	0.292		**0.758**	0.423
Flavobacterium frigoris ps1					
4NUH	**0.659**	0.446	**0.530**	**0.624**	**0.624**
Leucosporidium					0.304*
5B5H	**0.676**	**0.649**	0.304	**0.669**	0.389
Typhula ishikariensis					
4DT5 - complex	**0.718**				
Rhagium inquisitor					
Chain A	**0.554**	0.373	0.458	**0.618**	
4-21 SS		0.459			
Chain B	**0.621**	0.318	**0.641**	**0.643**	
4-21 SS		0.366			

Values given in bold distinguish the status of hydrophobic core recognised as disordered (not accordant with the idealised distribution).

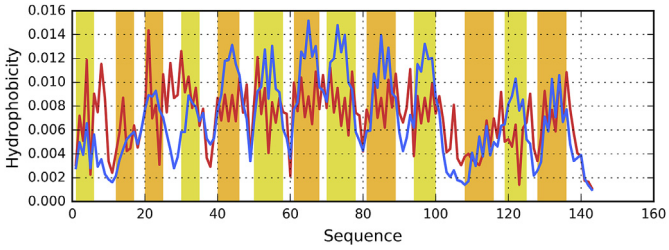

Fig. 9. Hydrophobicity distribution in 4DT5-A with N- and C- terminal fragments highlighted (black vertical lines). Theoretical distribution – blue line, observed distribution – red line. Fragments belonging to either β-sheet are colored yellow and orange respectively. The solenoid fragment corresponds to the central section, bracketed by vertical bars.

distribution also expose hydrophobic patches to which the water environment must adapt. Their high RD values indicate that the distribution of charge (and, consequently, their relationship with the environment) varies significantly.

Arguably the most interesting case involves proteins which include solenoid fragments. A solenoid is an ordered geometric form which results from cyclical propagation of a given secondary motif along a predetermined axis. In such circumstances, a monocentric hydrophobic core cannot emerge – rather, the structure reflects linear propagation of local minima and maxima in a direction determined by the solenoid's axis of elongation. Consequently, the surrounding water environment also forms "bands": where hydrophilicity is exposed, the structuralization of water is dominated by electrostatic effects, while molecules adjacent to hydrophilic fragments adopt a different (though as yet undetermined) structure, possibly involving levitation [65]. The resulting variable structuralization does not promote formation of ice crystals. We believe that this interpretation explains the antifreeze properties exhibited by all presented proteins, irrespective of their size and sequence.

Since linear propagation does not self-terminate, proteins which contain solenoid fragments also require suitable "stop" signals (or "caps"). Such caps are indeed found in the terminal sections of solenoids, where their local compliance with the fuzzy oil drop model prevents unbounded elongation.

A distinct subgroup of solenoid-like antifreeze proteins consists of proteins which, in addition to a solenoid fragment, include a parallel helix. These helices are usually highly accordant with the theoretical distribution of hydrophobicity, indicating that they may contribute to the solubility of the whole system. Note that complexation or binding of antifreeze proteins to other molecules (or membranes) would hamper their activity – given that antifreeze proteins require a water environment to perform their function.

Linear propagation of alternating hydrophobicity maxima/minima has also been studied in the context of amyloid fibrils. Amyloid structures listed in protein databases lack suitable "stop" signals and are therefore capable of unlimited propagation. With regard to solenoids, the "stop" signal usually assumes the form of an amphipathic helix, whose one side is naturally hydrophilic while the opposite side matches the local hydrophobicity distribution present in the solenoid.

The putative capability of antifreeze proteins to bind ice crystals is discussed in numerous publication [13,16,17,45,46]. Our analysis introduces an alternative mechanism, whereby the protein performs its function by disrupting the natural ordering of water in its proximity, preventing crystals from forming in the first place. Reports which mention levitation of water molecules above the hydrophobic surface [65] provide evidence for this alternative hypothesis. While the resulting structuralization of water is not precisely known, it is likely chaotic (Fig. 10). Exposure of alternating hydrophilic and hydrophobic residues on the protein surface may exert a significant effect on the water environment, even at a certain distance from the protein. Fig. 10 schematically illustrates the presented mechanism as it applies to various antifreeze proteins listed in this work.

The role of water molecules has also been discussed in the context of protein-ligand complexation [66,67].

In light of the fuzzy oil drop model, local exposure of hydrophobic and hydrophilic residues produces an ordering of the

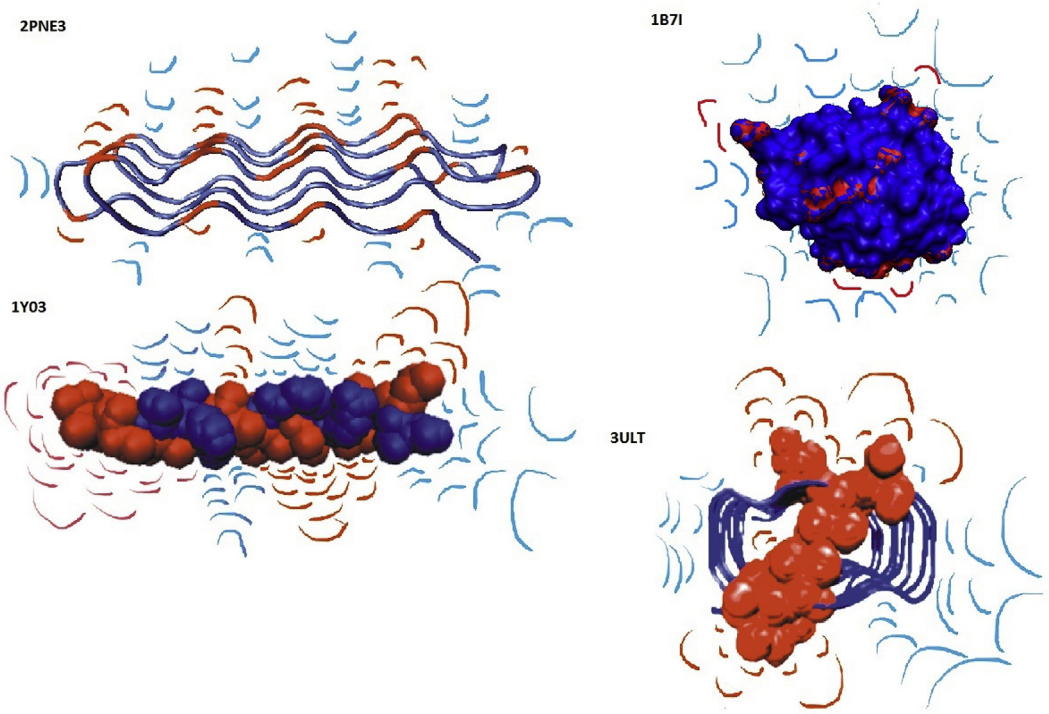

Fig. 10. Propagation of a diversified "hydrophobic" field depending on the internal hydrophobicity distribution in antifreeze proteins with various tertiary conformations (2PNE – amyloid-like protein; 1B7I – small globular protein consistent with the FOD model; 3ULT – solenoid with notable linear distribution of local hydrophobicity maxima/minima; 1Y03 – helical polypeptide with variable hydrophobicity). The red and blue wavelike patterns represent the proteins' influence on the water environment.

surrounding water molecules which, while unknown, differs from natural conditions. This is schematically illustrated in Fig. 10. The effect is particularly pronounced in the case of solenoid fragments, which expose alternating hydrophobicity minima/maxima and cause the surrounding water to adopt similar "bandlike" patterns, counteracting formation of ice crystals.

The authors of [68] express surprise at the observed antifreeze properties of saccharides and lipids, which are clearly incapable of docking other molecules (such as ice crystals). In contrast, the fuzzy oil drop model readily explains this phenomenon by noting the effect of surface charge distribution on the surrounding water particles [69]. Likewise, the reported high mobility of water on the ice-binding surface of hyperactive antifreeze proteins is fully consistent with the fuzzy oil drop model [70,71]. As shown in Fig. 10 the differing reaction of water to hydrophobic and hydrophilic residues may result in high mobility, induced by preferential interaction with polar groups and avoidance of hydrophobic residues.

The effects of antifreeze proteins are known to be amplified under high concentrations. The fuzzy oil drop model regards this as a result of increased disruption of the natural structuralization of water, which prevents ice crystals from forming [72]. While the interpretation illustrated in Fig. 10 appears naïve, it may be justified given the lack of a suitable theory explaining the structural properties of water in natural conditions and in the proximity of protein surfaces (including levitation effects [65]).

Acknowledgements

Many thanks to Piotr Nowakowski and Anna Śmietańska for technical support. The work was financially supported by Jagiellonian University Medical College grant no. K/ZDS/006363.

References

[1] J.D. Bernal, R.H. Fowler, A theory of water in ionic solutions, with particular reference to hydrogen and hydroxyl ions, J. Chem. Phys. 1 (1933) 515–548.
[2] L.G. Macdowell, E. Sanz, C. Vega, J.L. Abascal, Combinatorial entropy and phase diagram of partially ordered ice phases, J. Chem. Phys. 121 (20) (2004) 10145–10158.
[3] L.G. Macdowell, E. Sanz, C. Vega, J.L. Abascal, Combinatorial entropy and phase diagram of partially ordered ice phases, J. Chem. Phys. 121 (20) (2004) 10145–10158.
[4] S.V. Lishchuk, T.V. Lokotosh, N.P. Malomuzh, Properties of the H-bond network for two-dimensional lattice water model, J. Chem. Phys. 122 (24) (2005) 244504.
[5] R.L. Fulton, The nonlinear dielectric behavior of water: comparisons of various approaches to the nonlinear dielectric increment, J. Chem. Phys. 130 (20) (2009) 204503.
[6] J.L. Aragones, L.G. MacDowell, C. Vega, Dielectric constant of ices and water: a lesson about water interactions, J. Phys. Chem. A 115 (23) (2011) 5745–5758.
[7] S. Jenkins, A. Restrepo, J. David, D. Yin, S.R. Kirk, Spanning QTAIM topology phase diagrams of water isomers W4, W5 and W6, Phys. Chem. Chem. Phys. 13 (24) (2011) 11644–11656.
[8] V. Petkov, Y. Ren, M. Suchomel, Molecular arrangement in water: random but not quite, J. Phys. Condens Matter 24 (15) (2012) 155102.
[9] J.F. Ouyang, R.P. Bettens, Modelling water: a lifetime enigma, Chim. (Aarau) 69 (3) (2015) 104–111.
[10] J.S.J. Tan, L. Zhang, F.C.H. Lim, D.W.L. Cheong, Interfacial properties and monolayer collapse of alkyl benzene sulfonate surfactant monolayers at the decane-water interface from molecular dynamics simulations, Langmuir 33 (18) (2017) 4461–4476.
[11] D. Dong, J.B. Hooper, D. Bedrov, Structural and dynamical properties of tetraalkyl ammonium bromide aqueous solutions: a molecular dynamics simulation study using a polarizable force field, J. Phys. Chem. B 121 (18) (2017) 4853–4863.
[12] A. Miskowiec, Z.N. Buck, F.Y. Hansen, H. Kaiser, H. Taub, M. Tyagi, S.O. Diallo, E. Mamontov, K.W. Herwig, On the structure and dynamics of water associated with single-supported zwitterionic and anionic membranes, J. Chem. Phys. 146 (12) (2017) 125102.
[13] P. Christopher, C.P. Garnham, R.L. Campbell, P.L. Davies, Anchored clathrate waters bind antifreeze proteins to ice, PNAS 108 (2011) 7363–7367.
[14] S.W. Phippen, C.A. Stevens, T.D. Vance, N.P. King, D. Baker, P.L. Davies, Multivalent display of antifreeze proteins by fusion to self-assembling protein cages enhances ice-binding activities, Biochemistry 55 (49) (2016)

6811–6820.
[15] L. Du, M. Betti, Identification and evaluation of cryoprotective peptides from chicken collagen: ice-growth inhibition activity compared to that of type I antifreeze proteins in sucrose model systems, J. Agric. Food Chem. 64 (25) (2016) 5232–5240.
[16] M. Bar Dolev, I. Braslavsky, P.L. Davies, Ice-binding proteins and their function, Annu. Rev. Biochem. 85 (2016) 515–542.
[17] C.J. Marshall, K. Basu, P.L. Davies, Ice-shell purification of ice-binding proteins, Cryobiology 72 (3) (2016) 258–263.
[18] A. Ben-Naim, Myths and verities in protein folding theories: from Frank and Evans iceberg-conjecture to explanation of the hydrophobic effect, J. Chem. Phys. 139 (16) (2013) 165105.
[19] M.J. Rosen, J.T. Kunjappu, Surfactants and Interfacial Phenomena, fourth ed., John Wiley & Sons, Hoboken, New Jersey, 2012, p. 1. ISBN 1-118-22902-9.
[20] N. Pawar, P. Kaushik, H.B. Bohidar, Hydrophobic hydration and anomalous diffusion of elastin in an ethanolic solution, Phys. Chem. Chem. Phys. 19 (21) (2017) 13994–14000.
[21] W. Kauzmann, Some factors in the interpretation of protein denaturation, Adv. Protein Chem. 14 (1959) 1–63.
[22] B. Kalinowska, M. Banach, L. Konieczny, I. Roterman, Application of divergence entropy to characterize the structure of the hydrophobic core in DNA interacting proteins, Entropy 17 (3) (2015) 1477–1507.
[23] B. Kobe, A.V. Kajava, When protein folding is simplified to protein coiling: the continuum of solenoid protein structure, Trends Biochem. Sci. 25 (10) (2000) 509–515.
[24] A.V. Kajava, U. Aebi, A.C. Steven, The parallel superpleated beta-structure as a model for amyloid fibrils of human amylin, J. Mol. Biol. 348 (2) (2005) 247–252.
[25] A.V. Kajava, J.M. Squire, D.A. Parry, Beta-structures in fibrous proteins, Adv. Protein Chem. 73 (2006) 1–15.
[26] A.V. Kajava, A.C. Steven, Beta-rolls, beta-helices, and other beta-solenoid proteins, Adv. Protein Chem. 73 (2006) 55–96.
[27] T. Di Domenico, E. Potenza, I. Walsh, R.G. Parra, M. Giollo, G. Minervini, D. Piovesan, A. Ihsan, C. Ferrari, A.V. Kajava, S.C. Tosatto, RepeatsDB: a database of tandem repeat protein structures, Nucleic Acids Res. 42 (Database issue) (2014) D352–D357.
[28] J. Jorda, T. Baudrand, A.V. Kajava, PRDB: protein repeat DataBase, Proteomics 12 (9) (2012) 1333–1336.
[29] A.V. Kajava, A.C. Steven, The turn of the screw: variations of the abundant beta-solenoid motif in passenger domains of Type V secretory proteins, J. Struct. Biol. 155 (2) (2006) 306–315.
[30] L. Haleva, Y. Celik, M. Bar-Dolev, N. Pertaya-Braun, A. Kaner, P.L. Davies, I. Braslavsky, Microfluidic cold-finger device for the investigation of ice-binding proteins, Biophys. J. 111 (6) (2016) 1143–1150.
[31] K. Basu, S.S. Wasserman, P.S. Jeronimo, L.A. Graham, P.L. Davies, Intermediate activity of midge antifreeze protein is due to a tyrosine-rich ice-binding site and atypical ice plane affinity, FEBS J. 283 (8) (2016 Apr) 1504–1515.
[32] R. Drori, P.L. Davies, I. Braslavsky, When are antifreeze proteins in solution essential for ice growth inhibition? Langmuir 31 (21) (2015) 5805–5811.
[33] E. Liepinsh, G. Otting, M.M. Harding, L.G. Ward, J.P. Mackay, A.D. Haymet, Solution structure of a hydrophobic analogue of the winter flounder antifreeze protein, Eur. J. Biochem. 269 (4) (2002) 1259–1266.
[34] A.H. Kwan, K. Fairley, P.I. Anderberg, C.W. Liew, M.M. Harding, J.P. Mackay, Solution structure of a recombinant type I sculpin antifreeze protein, Biochemistry 44 (6) (2005) 1980–1988.
[35] S.H. Shah, R.K. Kar, A.A. Asmawi, M.B. Rahman, A.M. Murad, N.M. Mahadi, M. Basri, R.N. Rahman, A.B. Salleh, S. Chatterjee, B.A. Tejo, A. Bhunia, Solution structures, dynamics, and ice growth inhibitory activity of peptide fragments derived from an antarctic yeast protein, PLoS One 7 (11) (2012) e49788.
[36] S.P. Graether, C.I. DeLuca, J. Baardsnes, G.A. Hill, P.L. Davies, Z. Jia, Quantitative and qualitative analysis of type III antifreeze protein structure and function, J. Biol. Chem. 274 (17) (1999) 11842–11847.
[37] Z. Jia, C.I. DeLuca, H. Chao, P.L. Davies, Structural basis for the binding of a globular antifreeze protein to ice, Nature 384 (6606) (1996) 285–288.
[38] F.D. Sönnichsen, C.I. DeLuca, P.L. Davies, B.D. Sykes, Refined solution structure of type III antifreeze protein: hydrophobic groups may be involved in the energetics of the protein-ice interaction, Structure 4 (11) (1996) 1325–1337.
[39] H. Kumeta, K. Ogura, Y. Nishimiya, A. Miura, F. Inagaki, S. Tsuda, NMR structure note: a defective isoform and its activity-improved variant of a type III antifreeze protein from Zoarces elongates Kner, J. Biomol. NMR 55 (2) (2013) 225–230.
[40] Y. Liu, Z. Li, Q. Lin, J. Kosinski, J. Seetharaman, J.M. Bujnicki, J. Sivaraman, C.L. Hew, Structure and evolutionary origin of Ca(2+)-dependent herring type II antifreeze protein, PLoS One 2 (6) (2007) e548.
[41] S. Rothemund, Y.C. Liou, P.L. Davies, E. Krause, F.D. Sönnichsen, A new class of hexahelical insect proteins revealed as putative carriers of small hydrophobic ligands, Structure 7 (11) (1999) 1325–1332.
[42] S. Guo, C.P. Garnham, S. Karunan Partha, R.L. Campbell, J.S. Allingham, P.L. Davies, Role of Ca^{2+} in folding the tandem β-sandwich extender domains of a bacterial ice-binding adhesin, FEBS J. 280 (22) (2013) 5919–5932.
[43] K. Miura, S. Ohgiya, T. Hoshino, N. Nemoto, T. Suetake, A. Miura, L. Spyracopoulos, H. Kondo, S. Tsuda, NMR analysis of type III antifreeze protein intramolecular dimer. Structural basis for enhanced activity, J. Biol. Chem. 276 (2) (2001) 1304–1310.
[44] Y. Nishimiya, H. Kondo, M. Takamichi, H. Sugimoto, M. Suzuki, A. Miura, S. Tsuda, Crystal structure and mutational analysis of Ca2+-independent type II antifreeze protein from longsnout poacher, Brachyopsis rostratus, J. Mol. Biol. 382 (3) (2008) 734–746.
[45] S.P. Graether, M.J. Kuiper, S.M. Gagné, V.K. Walker, Z. Jia, B.D. Sykes, P.L. Davies, Beta-helix structure and ice-binding properties of a hyperactive antifreeze protein from an insect, Nature 406 (6793) (2000) 325–328.
[46] E.K. Leinala, P.L. Davies, Z. Jia, Crystal structure of beta-helical antifreeze protein points to a general ice binding model, Structure 10 (5) (2002) 619–627.
[47] M.E. Daley, L. Spyracopoulos, Z. Jia, P.L. Davies, B.D. Sykes, Structure and dynamics of a beta-helical antifreeze protein, Biochemistry 41 (17) (2002) 5515–5525.
[48] E.K. Leinala, P.L. Davies, D. Doucet, M.G. Tyshenko, V.K. Walker, Z. Jia, A beta-helical antifreeze protein isoform with increased activity. Structural and functional insights, J. Biol. Chem. 277 (36) (2002) 33349–33352.
[49] S.P. Graether, S.M. Gagné, L. Spyracopoulos, Z. Jia, P.L. Davies, B.D. Sykes, Spruce budworm antifreeze protein: changes in structure and dynamics at low temperature, J. Mol. Biol. 327 (5) (2003) 1155–1168.
[50] C. Li, X. Guo, Z. Jia, B. Xia, C. Jin, Solution structure of an antifreeze protein CfAFP-501 from Choristoneura fumiferana, J. Biomol. NMR 32 (3) (2005) 251–256.
[51] B.L. Pentelute, Z.P. Gates, V. Tereshko, J.L. Dashnau, J.M. Vanderkooi, A.A. Kossiakoff, S.B. Kent, X-ray structure of snow flea antifreeze protein determined by racemic crystallization of synthetic protein enantiomers, J. Am. Chem. Soc. 130 (30) (2008) 9695–9701.
[52] C.P. Garnham, R.L. Campbell, P.L. Davies, Anchored clathrate waters bind antifreeze proteins to ice, Proc. Natl. Acad. Sci. U. S. A. 108 (18) (2011) 7363–7367.
[53] A.J. Middleton, C.B. Marshall, F. Faucher, M. Bar-Dolev, I. Braslavsky, R.L. Campbell, V.K. Walker, P.L. Davies, Antifreeze protein from freeze-tolerant grass has a beta-roll fold with an irregularly structured ice-binding site, J. Mol. Biol. 416 (5) (2012) 713–724.
[54] J.H. Lee, A.K. Park, H. Do, K.S. Park, S.H. Moh, Y.M. Chi, H.J. Kim, Structural basis for antifreeze activity of ice-binding protein from arctic yeast, J. Biol. Chem. 287 (14) (2012) 11460–11468.
[55] H. Kondo, Y. Hanada, H. Sugimoto, T. Hoshino, C.P. Garnham, P.L. Davies, S. Tsuda, Ice-binding site of snow mold fungus antifreeze protein deviates from structural regularity and high conservation, Proc. Natl. Acad. Sci. U. S. A. 109 (24) (2012) 9360–9365.
[56] Y. Hanada, Y. Nishimiya, A. Miura, S. Tsuda, H. Kondo, Hyperactive antifreeze protein from an Antarctic sea ice bacterium Colwellia sp. has a compound ice-binding site without repetitive sequences, FEBS J. 281 (16) (2014) 3576–3590.
[57] H. Do, S.J. Kim, H.J. Kim, J.H. Lee, Structure-based characterization and antifreeze properties of a hyperactive ice-binding protein from the Antarctic bacterium Flavobacterium frigoris PS1, Acta Crystallogr. D. Biol. Crystallogr. 70 (2014) 1061–1073.
[58] J. Cheng, Y. Hanada, A. Miura, S. Tsuda, H. Kondo, Hydrophobic ice-binding sites confer hyperactivity of an antifreeze protein from a snow mold fungus, Biochem. J. 473 (2016) 4011–4026.
[59] A. Hakim, J.B. Nguyen, K. Basu, D.F. Zhu, D. Thakral, P.L. Davies, F.J. Isaacs, Y. Modis, W. Meng, Crystal structure of an insect antifreeze protein and its implications for ice binding, J. Biol. Chem. 288 (17) (2013) 12295–12304.
[60] T.A.P. de Beer, K. Berka, J.M. Thornton, R.A. Laskowski, PDBsum additions, Nucleic Acids Res. 42 (2014) D292–D296.
[61] M. Levitt, A simplified representation of protein conformations for rapid simulation of protein folding, J. Mol. Biol. 104 (1976) 59–107.
[62] S. Kullback, R.A. Leibler, On information and sufficiency, Ann. Math. Stat. 22 (1951) 79–86.
[63] S.N. Patel, S.P. Graether, Increased flexibility decreases antifreeze protein activity, Protein Sci. 19 (2010) 2356–2365.
[64] M. Banach, B. Kalinowska, L. Konieczny, I. Roterman, Role of disulfide bonds in stabilizing the conformation of selected enzymes—an approach based on divergence entropy applied to the structure of hydrophobic core in proteins, Entropy 18 (3) (2016) 67.
[65] T.M. Schutzius, S. Jung, T. Maitra, G. Graeber, M. Köhme, D. Poulikakos, Spontaneous droplet trampolining on rigid superhydrophobic surfaces, Nature 527 (7576) (2015) 82–85.
[66] C.M. Labbé, T. Pencheva, D. Jereva, D. Desvillechabrol, J. Becot, B.O. Villoutreix, I. Pajeva, M.A. Miteva, AMMOS2: a web server for protein-ligand-water complexes refinement via molecular mechanics, Nucleic Acids Res. (2017), https://doi.org/10.1093/nar/gkx397.
[67] S. Heiles, R.J. Cooper, M.J. DiTucci, E.R. Williams, Sequential water molecule binding enthalpies for aqueous nanodrops containing a mono-, di- or trivalent ion and between 20 and 500 water molecules, Chem. Sci. 8 (4) (2017) 2973–2982.
[68] K.R. Walters Jr., A.S. Serianni, T. Sformo, B.M. Barnes, J.G. Duman, A nonprotein thermal hysteresis-producing xylomannan antifreeze in the freeze-tolerant Alaskan beetle Upis ceramboides, PNAS 106 (48) (2009) 20210–20215.
[69] J.G. Duman, Animal ice-binding (antifreeze) proteins and glycolipids: an overview with emphasis on physiological function, J. Exp. Biol. 218 (2015) 1846–1855.
[70] K. Modig, J. Qvist, C.B. Marshall, P.L. Davies, B. Halle, High water mobility on the ice-binding surface of a hyperactive antifreeze protein, Phys. Chem. Chem. Phys. 12 (35) (2010) 10189–10197.
[71] A. Miskowiec, Z.N. Buck, F.Y. Hansen, H. Kaiser, H. Taub, M. Tyagi, S.O. Diallo,

E. Mamontov, K.W. Herwig, On the structure and dynamics of water associated with single-supported zwitterionic and anionic membranes, J. Chem. Phys. 146 (12) (2017) 125102.

[72] S. Mahatabuddin, Y. Hanada, Y. Nishimiya, A. Miura, H. Kondo, P.L. Davies, S. Tsuda, Concentration-dependent oligomerization of an alpha-helical antifreeze polypeptide makes it hyperactive, Sci. Rep. 7 (2017) 42501.